J Appl Electrochem (2010) 40:885–902
DOI 10.1007/s10800-009-9938-7

ORIGINAL PAPER

Recent developments and trends in the electrochemical promotion of catalysis (EPOC)

A. Katsaounis

Received: 8 January 2009 / Accepted: 28 May 2009 / Published online: 26 June 2009

Abstract Electrochemical Promotion of Catalysis (EPOC or NEMCA effect) is one of the most exciting discoveries in Electrochemistry with great impact on many catalytic and electrocatalytic processes. According to the words of John O'M. Bockris, EPOC is a triumph, and the latest in a series of advances in electrochemistry which have come about in the last 30 years. It has been shown with more than 80 different catalytic systems that the catalytic activity and selectivity of conductive catalysts deposited on solid electrolytes can be altered in a very pronounced, reversible and, to some extent, predictable manner by applying electrical currents or potentials (typically up to ±2 V) between the catalyst and a second electronic conductor (counter electrode) also deposited on the solid electrolyte. The induced steady-state change in catalytic rate can be up to 135×10^3% higher than the normal (open-circuit) catalytic rate and up to 3×10^5 higher than the steady-state rate of ion supply. EPOC studies in the last 7 years mainly focus on the following four areas: Catalytic reactions with environmental impact (such as reduction of NO_x and oxidation of light hydrocarbons), mechanistic studies on the origin of EPOC (using mainly oxygen ion conductors), scale-up pf EPOC reactors for potential commercialization via development of novel compact monolithic reactors and application of EPOC in high or low temperature fuel cells via introduction of the concept of triode fuel cell. The most recent EPOC studies in these areas are discussed in the present review and some of the future trends and aims of EPOC research are presented.

A. Katsaounis (✉)
Department of Environmental Engineering, Technical University of Crete, 73100 Chania, Greece
e-mail: alex.katsaounis@enveng.tuc.gr

Keywords EPOC · NEMCA · Electrochemical promotion · Electropromotion

List of acronyms

AP	Atmospheric pressure
BCN	$Ba_3Ca_{1.19}Nb_{1.82}O_{9-a}$
BPG	Gd-doped $BaPrO_3$
BZY	Y-doped $BaZrO_3$
CV	Cyclic voltammetry
EP	Electrochemical promotion
EPOC	Electrochemical promotion of catalysis
FC	Fuel cell
FTIR	Fourier transform infrared spectroscopy
HC	Hydrocarbon
HV	High vacuum
LaAlO	$La_{1.8}Al_{0.2}O_3$
LSC	$La_{0.6}Sr_{0.4}Co_{0.2}F_{0.8}O_3$
LSCM	$La_{0.8}Sr_{0.2}Co_{0.8}Fe_{0.2}O_3$
LSM	$La_{0.85}Sr_{0.15}MnO_3$
LSV	Linear sweep voltammetry
MEPR	Monolithic electropromoted reactor
MSI	Metal-support interactions
NASICON	$Na_3Zr_2Si_2PO_{12}$
NEMCA	Non-Faradaic elecrochemical modification of catalytic activity
PEMFC	Polymer electrolyte membrane fuel cell
PVD	Physical vapour deposition
RWGS	Reversed water-gas-shift
SCY	$SrCe_{0.95}Y_{0.05}O_{3-a}$
SEM	Scanning electron microscopy
SEM-EDX	Energy-dispersive X-ray spectroscopy analysis conducted by means of SEM
SOFC	Solid oxide fuel cell
STM	Scanning tunnelling microscopy

SZY	$SrZr_{0.95}Y_{0.05}O_{3-a}$
TE	Transient experiments
tpb	Three phase boundaries
TPD	Temperature programmed desorption
TPR	Temperature programmed reaction
UHV	Ultra high vacuum
WGS	Water-gas-shift
YSZ	Y_2O_3-doped ZrO_2

1 Introduction

The group of Vayenas at MIT in the early eighties [1] first reported that the catalytic activity and selectivity of conductive catalysts deposited on solid electrolytes can be altered in a very pronounced, reversible and, to some extent, predictable manner by applying electrical currents or potentials (typically up to ±2 V) between the catalyst and a second electronic conductor (counter electrode) also deposited on solid electrolyte. In addition to this group which reported EPOC, the groups of Sobyanin [2], Comninellis [3], Lambert [4], Haller [5], Anastasijevic [6], Stoukides [7], Yentekakis [8], Smotkin [9], Tsiakaras [10], Imbihl [11], Pacchioni [12], Bjerrum [13], Lee [14], Metcalfe [15], Janek [16], Barbier [17], Leiva [18] and more recently the groups of Vernoux [19], and Jose Luis Valverde [20, 21] have also made significant contributions in this area while the importance of EPOC in electrochemistry, surface science and heterogeneous catalysis has been discussed by Bockris [22], Wieckowski [23], Pritchard [24], Haber [25] and Riess [26, 27] respectively. Electrochemical Promotion of Catalysis (EPOC or NEMCA effect) with ionically conducting (Y_2O_3-stabilized-ZrO_2, YSZ) or mixed ionic-electronic conductors (ZrO_2, CeO_2, TiO_2, W^{6+}-doped-TiO_2) is a phenomenon of Electrocatalysis which affects the chemisorptive and catalytic properties of metal or metal oxide catalysts in a very pronounced manner [28]. The term Electrochemical Promotion (EP) is used to describe the very pronounced changes observed in the catalytic properties of conductive catalysts deposited on solid electrolytes upon application of electrical currents or potentials. The metal catalyst is usually in the form of a porous and electronically conducting film deposited on the solid electrolyte (e.g. O^{2-} or mixed O^{2-}-electronic conductor). Either single chamber or fuel cell type configurations can be used for EPOC studies [28]. In the former case all electrodes are exposed in the gas mixture while in the second configuration only the working electrode is in contact with the reactants.

For the case of O^{2-} conductor supports, the origin of EPOC has been found to stem from the migration (reverse spillover) of anionic $O^{\delta-}$ species from the support to the metal–gas interface (Fig. 1a). These electrochemically assisted backspillover of the $O^{\delta-}$ species, together with their image charge in the metal create an overall neutral double layer at the metal–gas interface and affect both chemisorption and catalysis in a pronounced manner. At high oxygen coverages the backspillover $O^{\delta-}$ species are distinct from, and more strongly adsorbed than, oxygen adsorbed from the gas phase [29–31]. They are also less reactive for catalytic oxidations than gas-supplied oxygen and thus act as sacrificial promoters [28]. Similar considerations apply when using other types of solid electrolytes, such as Na^+ conductors (Fig. 1b). The above mechanism is evident from Fig. 2 which shows the general behaviour of oxygen adsorption on polycrystalline Pt deposited on O^{2-} solid electrolytes, such as YSZ. Temperature Programmed Desorption (TPD) of oxygen under Ultra High Vacuum (UHV) conditions has been used extensively to study the difference of non-stoichiometric lattice oxygen from oxygen originating from the gas phase [28–32]. Figure 2a presents the O_2 TPD spectra on Pt/YSZ when oxygen is supplied from the gas phase. One observes a broad oxygen peak (β_2 state) after catalyst exposure to oxygen atmosphere. In Fig. 2b oxygen has been supplied electrochemically in the form of oxygen ions (O^{2-}) from the support, YSZ, using an external circuit and a constant positive current. Nonstoichiometric oxygen [30] from the support

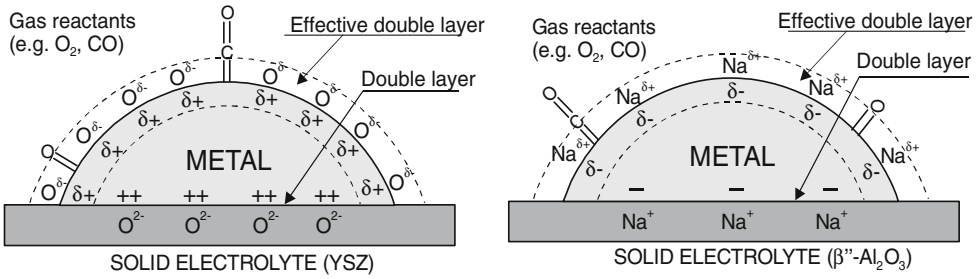

Fig. 1 Schematic representation of a metal electrode deposited on a O^{2-} conducting (*left*) and on a Na^+ conducting (*right*) solid electrolyte, showing the location of the metal-electrolyte double layer and of the effective double layer created at the metal–gas interface due to potential-controlled ion migration (backspillover) [28]. The interaction is also depicted between the effective double layer and the adsorbed reactants during CO oxidation. Reprinted with permission from Kluwer Academic/Plenum Publishers

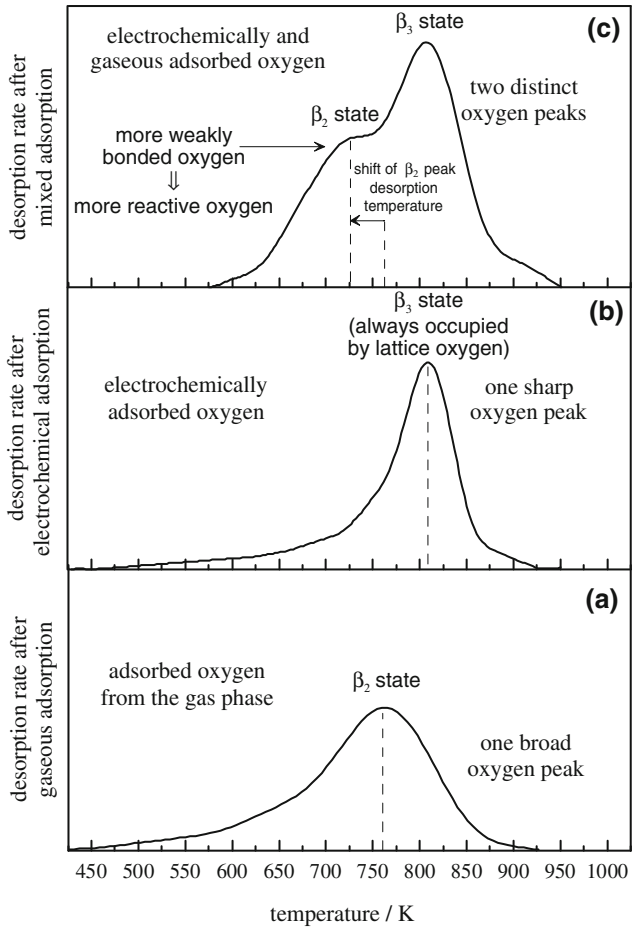

Fig. 2 General behaviour of oxygen thermal desorption spectra from Pt thin films deposited on YSZ after oxygen adsorption at high temperatures (>200 °C) and medium heating rates (0.5–1.5 °C/s). **a** gaseous adsorption, **b** electrochemical adsorption and **c** mixed adsorption. Based on [28]

migrates and gets adsorbed on the catalyst surface. The result is a spectrum with one sharp oxygen peak (β_3 state) desorbing at higher temperatures than the β_2 state. This confirms the assumption that the backspillover oxygen is more strongly adsorbed on the surface than the gaseous oxygen of β_2 state. If we try to carry out a mixed adsorption experiment (from the gas phase and electrochemically, using a constant positive current) we can simulate the conditions of Electrochemical Promotion where the catalyst is exposed to an oxygen containing atmosphere (for oxidation reactions) and at the same time O^{2-} is supplied to the catalyst surface from YSZ support. Under these conditions we observe the behaviour shown in Fig. 2c. Two distinct oxygen peaks appear, a broad one originating from the gas phase (β_2 state) and a sharper one (β_3 state) occupied by a more strongly bonded oxygen. It is worth noting that the β_3 state which corresponds to the backspillover oxygen species acts as a promoter for supplied oxygen since the last one moves to more weakly (and as a result more reactive) bonded states on the catalyst surface (lower desorption temperatures). More detailed discussion about the above mechanism of electrochemical promotion can be found elsewhere [29–31]. Figures 3 and 4 present results of the basic phenomenology of EPOC when using O^{2-} and H^+ conducting supports respectively. In the former case (Fig. 3) the (usually porous) metal (Pt) catalyst-electrode, typically 40 nm to 4 μm thick, is deposited on an 8 mol% Y_2O_3- stabilized-ZrO_2 solid electrolyte during ethylene oxidation [33]. In the latter case (Fig. 4) the nanodispersed Pd/C catalyst is deposited on porous conductive graphitic C which is supported on Nafion, a H^+ conductor, during 1-butene hydrogenation and isomerization [9]. In both cases under open-circuit operation ($I = 0$, no electrochemical rate) there is a catalytic rate, r_o, of ethylene consumption for oxidation to CO_2 (Fig. 3) or of 1-butene consumption due to reduction to butane and isomerization to cis-2-butene and trans-2-butene (Fig. 4). Application of an electrical current, I, or potential, U_{WR}, between the catalyst and a counter electrode and thus changing the catalyst potential, U_{WR}, with respect to a reference

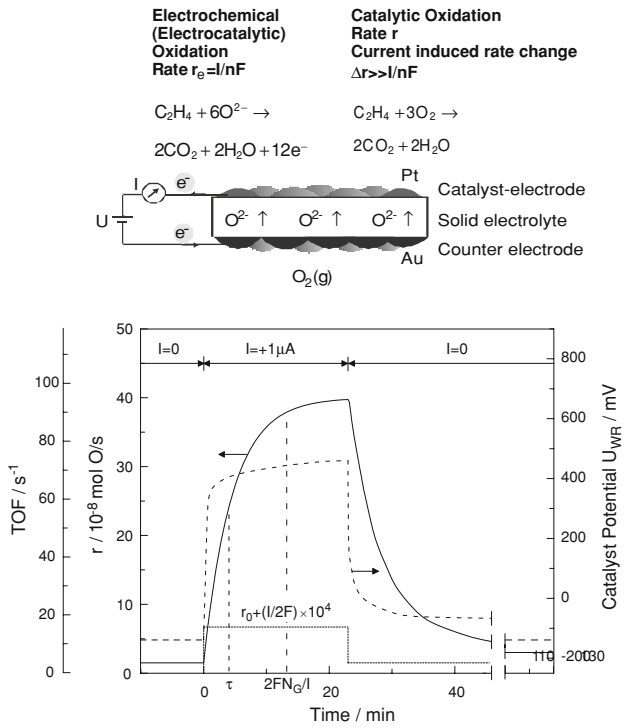

Fig. 3 Basic experimental setup and operating principle of electrochemical promotion with O^{2-} conducting supports (*up*). Catalytic rate r and turnover frequency TOF response of C_2H_4 oxidation on Pt deposited on YSZ, an O^{2-} conductor upon step changes in applied current (*down*) [33]. $T = 370$ °C, $P_{O_2} = 4.6$ kPa, $P_{C_2H_4} = 0.36$ kPa. Also shown (*dashed line*) the catalyst-electrode potential U_{WR} response with respect to the reference R electrode. N_G is the Pt/gas interface surface area, in mol Pt, and TOF is the catalytic turnover frequency (mol O reacting per surface Pt mol/s). Reprinted with permission from Elsevier

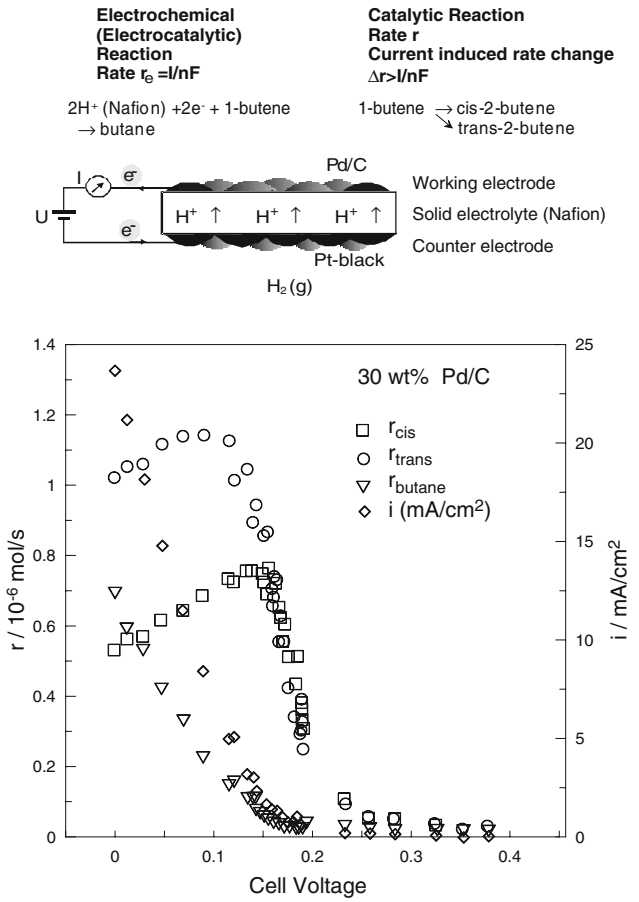

Fig. 4 Basic experimental setup and operating principle of electrochemical promotion with H^+ conducting supports (*up*). Electrochemical Promotion of an isomerization reaction (*down*) [9]. Steady state effect of cell potential on the cell current I and on the rates of formation of cis-2-butene, trans-2-butene and butane produced from 1-butene supplied over a dispersed Pd/C catalyst-electrode, deposited on Nafion, a H^+ conductor at room temperature. Reprinted with permission from [9]. Copyright (1997) American Chemical Society

electrode, causes very pronounced and strongly non-Faradaic (i.e. $\Delta r \gg I/2F$ in Fig. 3, $\Delta r \gg |-I/F|$ in Fig. 4) alterations both to the catalytic rate (Figs. 3 and 4) and to the product selectivity (Fig. 4). Two parameters are commonly used to describe the magnitude of EPOC:

1. The apparent Faradaic efficiency, Λ:

$$\Lambda = \Delta r_{catalytic}/(I/nF) \quad (1)$$

where $\Delta r_{catalytic}$ is the current-or potential-induced change in catalytic rate, I is the applied current, n is the charge of the applied ion and F is the Faraday's constant.

2. The rate enhancement, ρ:

$$\rho = r/r_o \quad (2)$$

where r is the electropromoted catalytic rate and r_o is the unpromoted (open-circuit) catalytic rate.

3. The promotion index, PI_j, where j is the promoting ion (e.g. O^{2-} for the case of YSZ or H^+ for the case of Nafion), defined from:

$$PI_j = (\Delta r/r_o)/\Delta\theta_j \quad (3)$$

where θ_j is coverage of the promoting ion on the catalyst surface.

A reaction exhibits electrochemical promotion when $|\Lambda| > 1$, while electrocatalysis is limited to $|\Lambda| \leq 1$. A reaction is termed *electrophobic* when $\Lambda > 1$ and *electrophilic* when $\Lambda < -1$. In the former case the rate increases with catalyst potential, U_{WR}, while in the latter case the rate decreases with catalyst potential. Λ values up to 3×10^5 and ρ values up to 150 [28] have been found for several systems. More recently ρ values between 300 [34, 35] and 1,400 [36, 37] have been observed for C_2H_4 and C_3H_8 oxidation on Pt/YSZ, respectively. In the experiment of Fig. 3 [33], $\Lambda = 74{,}000$ and $\rho = 26$, i.e. the rate of C_2H_4 oxidation increases by a factor of 25 while the increase in the rate of O consumption is 74,000 times larger than the rate, I/2F, of O^{2-} supply to the catalyst. In the experiment of Fig. 4 [9] the maximum ρ values for the production of cis-2-butene, trans-2-butene and butane are of the order of 50 and the corresponding maximum Λ values are of the order of 40 for cis-2-butene formation, 10 for trans-2-butene formation and less than one for butane formation. Thus, each proton supplied to the Pd catalyst can cause the isomerization of up to 40 1-butene molecules to cis-2- butene and up to 10 1-butene molecules to trans-2-butene while the hydrogenation of 1-butene to butane is electrocatalytic, i.e. Faradaic.

Until now (end of 2008), numerous different catalytic reactions (oxidations, reductions, hydrogenations, dehydrogenations, isomerizations, decompositions) have been electrochemically promoted on Pt, Pd, Rh, Ag, Au, Ni, Cu, Fe, IrO_2, RuO_2 catalysts deposited on O^{2-} (YSZ), Na^+ or K^+ (β''-Al_2O_3), H^+ ($CaZr_{0.9}In_{0.1}O_{3-a}$, Nafion), F^- (CaF_2), aqueous, molten salt and mixed ionic-electronic (TiO_2), CeO_2 conductors. EPOC seems to be not limited to any particular class of conductive catalyst, catalytic reaction or ionic support. It can be used in order to affect the rate and selectivity of heterogeneous catalytic reactions in a reversible and very pronounced manner. This non-Faradaic activation of heterogeneous catalytic reactions is a novel and promising application of electrochemistry with several technological possibilities, particularly in industrial product selectivity modification and in exhaust gas treatment. In the next paragraphs a thorough review will be given on the most recent achievements (from 2002 till now, e.g. after the publication of the first book of Electrochemical Promotion of Catalysis in 2001 [28]) in the field of EPOC. In this 7-year period numerous studies have been reported

mainly focusing on the following areas: effectiveness of EPOC on specific catalytic reactions with environmental or industrial interest (such as reduction of NO_x and oxidation of light hydrocarbons), mechanistic studies and investigation of the origin of EPOC (using mainly oxygen ion conductors), commercialization of EPOC (via developing novel compact monolithic reactors and minimizing the required electrical connections) and application of EPOC in high or low temperature fuel cell devices (via introduction of the triode fuel cell concept).

2 Electrochemical promotion of reactions with environmental and industrial impact

From the early studies of EPOC, almost three decades ago reactions with environmental and industrial impact attract the attention of many scientific groups. The scientific focus on light hydrocarbon oxidations and various oxides reductions becomes nowadays more intensive mainly due to the strict emissions laws established in most countries. The first category of oxidations includes hydrocarbons such as CH_4 [38], C_2H_4 [39–41], C_3H_6 [19, 21, 42–45], C_3H_8 [19, 36, 37, 45–50], alcohols [10, 51] and CO [52] while the reduction of NO_x mainly with hydrocarbons under lean burn conditions is the subject of numerous reports [53–58]. Several studies also focused on hydrogenations (such as C_2H_5OH hydrogenation [10, 51]), on the water gas shift (WGS) and reverse WGS reactions [59, 60] and on NH_3 decomposition [61]. Table 1 presents all studies carried out during the last 7 years. EPOC have been found to have great impact both in catalytic rate and in selectivity of the above reactions. We could see as an example the case of propane combustion over Pt/YSZ electrocatalyst (Fig. 5). This reaction was investigated by Bebelis and Kotsionopoulos [36] who found that under relatively reducing conditions and high temperatures (>450 °C), constant application of positive current ($I = 3.5$ mA) causes at steady state a dramatic increase of catalytic rate up to 135×10^3% ($\rho = r/r_o = 1350$). The rate increase ($\Delta r = r - r_o = 2560 \times 10^{-9} - 1.9 \times 10^{-9} = 2558 \times 10^{-9}$ molO/s) was 141 times larger than the rate I/2F of O^{2-} supply to the Pt catalyst ($I/2F = 18.14 \times 10^{-9}$ molO/s). Under the same reactant composition electropromotion has been also observed after negative polarization too. Rate enhancements ratios up to 1130 have been reported [36] when O^{2-} was removed from the catalyst to the solid electrolyte. The phenomenon of promotion in this case is fully reversible since the catalytic rate reaches its initial value after current interruption (Fig. 5). The observed electrochemical promotion behaviour can be rationalized in the frame of the general considerations used to explain the NEMCA effect [24, 28], in view of the mechanism of the reaction and the relative strength of the chemisorptive bonds of the adsorbed reactants. When the temperature is high enough ([36], Fig. 5) and the P_{O_2}/P_{HC} ratio is lower than the stoichometric ratio, the coverages of the reactants can be assumed to be relatively low, with HC (in this case C_3H_8) coverage being much lower than oxygen coverage as both reactants compete for the same sites and oxygen is more strongly adsorbed on metal surfaces compared to many HC (like CH_4 or C_3H_8). Thus, either positive or negative overpotential application is expected to enhance the rate [28, 62] as it will enhance chemisorption and increase coverage of either hydrocarbon (electron donor) or oxygen (electron acceptor), respectively. Oxygen is more strongly adsorbed; thus, weakening of its chemisorptive bond upon application of positive overpotentials is in general expected to have the most significant impact on the rate (Fig. 5). The above explanation takes into account the rules of the promotion established some years ago by the group of Vayenas [62–64]. Using these rules the observed electropromotion behaviour of catalytic reactions can be explained while useful information can be drawn about the type of promoter which is required for the promotion.

Despite the fact that YSZ is mainly used as the solid electrolyte and Pt films as the catalyst-working electrode, other metals or metal oxides deposited on solid electrolytes with O^{2-}, H^+, K^+, Na^+ conductivity are also under investigation. Methane oxidation was studied by Roche et al. [38] using Pd on YSZ prepared by physical vapour deposition (PVD) where under positive polarization Faradaic efficiencies up to 258 and rate enhancement ratios up to 50 were observed. Propene oxidation is another reaction studied using various working electrodes deposited on several solid electrolytes. The results reported by the group of Vernoux [19, 21, 42, 44, 45] in Lyon reveal the usefulness of β''-Al_2O_3 (with K^+ conductivity) and NASICON (a Na^+ conductor) besides YSZ as solid electrolytes in conjunction with Pt working electrodes. In all cases electrophilic behaviour was observed under constant applied current or potentials. The behaviour of the reaction (propene oxidation) remains the same (electrophilic) even if the catalytic electrode is changed from a metal (like Pt) to a perovskite like LSCM ($La_{0.8}Sr_{0.2}Co_{0.8}Fe_{0.2}O_3$) as reported by Gaillard et al. [43]. On the other hand totally different behaviour can be observed during oxidation of saturated hydrocarbons like propane. Using various types of electrocatalysts (LSM/YSZ [46], Pt/YSZ [19, 37, 45, 47], Rh/YSZ [36, 49], Pd/YSZ [65], Ag/YSZ [50], Pt/ β''-Al_2O_3 (with Na^+ conductivity) [48]) it has been found that the reaction exhibits purely electrophobic or in some cases (depending on the reaction conditions) inverted volcano behaviour.

In addition to oxidations, reductions are also one of the main applications of EPOC. More specifically NO reduction by hydrocarbons like C_2H_4 or C_3H_6 was the subject of

Table 1 Studies of electrochemical promotion of catalysis reported between 2002 and 2008 using various catalyst-working electrodes and solid electrolytes

Electrochemical Promotion of reactions with environmental and industrial interest

Reactants	Reaction type	Electrocatalyst	Type of conductor	General behaviour under EP conditions	References
CH_4, O_2	Oxidation	Pd/YSZ/Au prepared by PVD technique	O^{2-}	Electrophobic behaviour with Λ values up to 258 and ρ values up to 50	[38]
CO_2, H_2	Hydrogenation	Pd/β''-Al_2O_3/Au Pd/YSZ/Au	Na^+	Non-faradaic increase induced in the rate of the water gas shift reaction at 533–605 °C and $2.1 < CO_2/H_2 < 3.5$	[99]
CO_2, H_2	Hydrogenation RWGS reaction	Cu/SZY/Pd (FC type configuration)	H^+	The whole process under electrocatalytic mode was sub-Faradaic. In all cases electrocatalytic rate were much higher than the catalytic one	[60]
CO_2, H_2	Hydrogenation	Rh/YSZ/Au	O^{2-}	O^{2-} on catalyst promote the production of CH_4 and minimize the CO production	[100]
CO, H_2O	WGS reaction	Pt/SZY/Pd	H^+	EP of H_2 production observed when protons pumped away from the catalyst (Pt). Λ values up to 8 and ρ values up to 2 reported	[59]
CO, O_2	Oxidation	Pt/β''-Al_2O_3/Au	K^+	Electrophilic behaviour. K^+ on the catalyst promote CO oxidation and cdecreases the light-off temperature	[52]
C_2H_4, O_2	Oxidation	Pt/BCN/Au	H^+	Electrophilic behaviour with Λ values up to 1000 and ρ values up to 12 under oxidizing conditions	[39]
C_2H_4, O_2	Oxidation	Pt/$BaZr_{0.9}Y_{0.1}O_{3-a}$/Pt	H^+	In oxidizing conditions, oxide ion conduction is pronounced, while in atmospheres with hydrogen-containing species proton conduction takes place. In both cases promotion of the reaction was observed	[40]
C_2H_4, O_2	Oxidation	Pt/BPG/Au and Pt/BZY/Au	H^+	Electropilic behaviour with small effect under polarization at low temperatures (<400 °C). BZY electrolyte shows quite good proton conductivity	[41]
C_2H_5OH, O_2	Oxidation, dehydrogenation	Pt/YSZ/Pt (FC type configuration)	O^{2-}	Electrophobic behaviour was observed with increase both in the acetaldehydeand the CO_2 production rate. Λ values for the reaction of ethanol dehydrogenation up to 10^4 were reported	[10, 51]
C_3H_6, O_2	Oxidation	Pt/YSZ/Au prepared by metal sputtering	O^{2-}	Electrophilic behaviour with Λ values up to 779 and ρ values lower than 1	[19, 42]
C_3H_6, O_2	Oxidation	Pt//β''-Al_2O_3/Au prepared by metal sputtering	K^+	Electrophilic behaviour with ρ values up to 6	[21]
C_3H_6, O_2	Oxidation	LSCM/YSZ/Au	O^{2-}	Electrophilic behaviour. The utilization of LSCM is restricted to oxidising atmospheres	[43]
C_3H_6, O_2	Oxidation	Pt/NASICON/Au prepared by sputtering	Na^+	Electrophilic behaviour with ρ values up to 3 near stoichiometry. No promotional effect under oxidizing conditions	[44, 45]
C_3H_8, O_2	Oxidation	Pt//β''-Al_2O_3/Au	Na^+	Electrophobic behaviour. Changes in the catalytic rate by up to 60 times larger than the corresponding change in sodium coverage	[48]
C_3H_8, O_2	Oxidation	Pt/YSZ/Au and Rh/YSZ/Au	O^{2-}	Inverted volcano behaviour. Non-Faradaic increases in catalytic rates with ρ values up to 4 for the case of Rh and up to 1350 for the case of Pt	[36, 49]
C_3H_8, O_2	Oxidation	Pt/YSZ/Au prepared by sputtering	O^{2-}	Electrophobic behaviour	[19, 45, 47]

Table 1 continued

Electrochemical Promotion of reactions with environmental and industrial interest

Reactants	Reaction type	Electrocatalyst	Type of conductor	General behaviour under EP conditions	References
C_3H_8, O_2	Oxidation	LSM/YSZ/Au	O^{2-}	Electrophobic behaviour with small effect of polarization. Λ decreases as the applied potential, the temperature and the thickness of the catalyst is increased	[46]
C_3H_8, O_2	Oxidation	Pt/YSZ/Ag, Pd/YSZ/Ag and Ag/YSZ/Ag	O^{2-}	Inverted volcano behaviour using Pt and Pd. Purely electrophobic using Ag. Three orders of magnitude larger catalytic rates observed under positive polarization using Pt/YSZ/Ag	[37, 50]
N_2O, C_3H_6, O_2, H_2O	Reduction	Pt/β''-Al_2O_3/Au	K^+	K^+ on catalyst promote the selective reduction of N_2O to N_2 and minimize the activity of O_2 and H_2O as poisons	[20, 101]
NO, C_3H_6, O_2	Reduction	Pt/YSZ/Au prepared by ESD technique	O^{2-}	Electrophilic behaviour	[53]
NO, C_3H_6, O_2	Reduction	Pt/β''-Al_2O_3/Au prepared by impregnation	Na^+	Electrophilic behaviour. The efficiency of the EP for NO removal decreases with oxygen concentration. Selectivity up to 70% observed under negative polarization	[55, 56]
NO, C_3H_6, O_2	Reduction	Ir/YSZ	O^{2-}	Electrophobic behaviour for NO and C_3H_6 consumption and enhancement of N_2 selectivity upon positive applied currents. N_2O production decreases both with negative and positive polirization	[54]
NO, C_3H_6, O_2	Reduction	Pt/NASICON/Au	Na^+	Under lean burn conditions EP shown to enhance strongly both the catalytic activity and the selectivity to N_2. Electrophilic behaviour for CO_2 and inverted volcano behaviour for N_2 production was observed at 295 °C	[57]
NO, C_3H_6, O_2	Reduction	Rh/YSZ/Au	O^{2-}	Inverted volcano behaviour for both CO_2 and N_2 with strongly non-Faradaic catalytic rates. Faradaic efficiencies up to 7,000 for CO_2 and 200 for N_2 formation and rate enhancement ratios up to 200 for CO_2 and 55 for N_2 were observed under positive polarization	[66]
NO, C_3H_6, O_2	Storage/reduction	Pt/β''-Al_2O_3/Au	K^+	NO_x is stored on the catalyst surface in form of potassium nitrates under negative polarization while under positive polarization, the catalyst is regenerated, and the stored nitrates are efficiently desorbed and reduced to N_2	[58]
NH_3	Decomposition	Ru/SCY/Ag	H^+	Inverted volcano behaviour. 75% decrease in the reaction activation energy under positive polarization	[61]
C_3H_8, H_2O	Decomposition	Pd/SCY/Pd (FC type configuration)	H^+	4-fold increase in the rate of propane decomposition was observed by increasing P_{H_2O} from 0.3 to 2.8 kpa. During the electrochemical pumping of hydrogen, the rate of hydrogen pumped to the outer chamber over I/2F reaches values up to 0.9	[65, 69]
H_2, O_2	H_2 oxidation	Pt–Ru/KOH (sol.)/Pt or Pt–Ru/$HClO_4$(sol.)/Pt reference: hydrogen electrode	Liquid electrolytes (pH: 2–13)	The kinetics of the catalytic oxidation of H_2 can be affected by electrochemical polarization of the electrolyte/electrode interface mainly under high pH values of the solution (high OH^- ionic conduction)	[102]

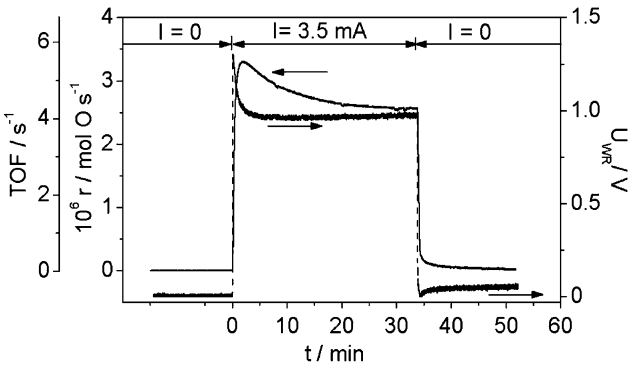

Fig. 5 Catalytic rate r, turnover frequency TOF, rate enhancement ratio r/r_o, Faradaic efficiency Λ and catalyst potential U_{WR} response to a step change in applied positive current. $T = 480$ °C, $P_{O_2} = 4.7$ kPa, $P_{C_3H_8} = 1.4$ kPa, flowrate 483 cm^3(STP)/min [36]. Reprinted with permission from Elsevier

many studies during the last 7 years [53–57, 66]. Propene is the most widely used hydrocarbon for the reduction of NO [53–57, 66]. Both electrophilic and electrophobic behaviour was observed depending on the electrocatalyst used and the reaction parameters. Using Pt/NASICON (Na^+ conductor) Vernoux et al. [57] found that under lean burn conditions EPOC enhances strongly both the catalytic activity and the selectivity to N_2. Electrophilic behaviour for CO_2 production and inverted volcano behaviour for N_2 production was observed at 295 °C. In another study of the same reaction Constantinou et al. [66] using Rh/YSZ/Au reported inverted volcano behaviour for both CO_2 and N_2 production with strongly non-Faradaic catalytic rates. Faradaic efficiencies up to 7000 for CO_2 and 200 for N_2 formation and rate enhancement ratios up to 200 for CO_2 and 55 for N_2 were observed under positive polarization and oxygen partial pressure up to 0.5 kPa [66]. In general catalytic activity and selectivity to N_2 decreases dramatically with O_2 concentration, something which could be counterbalanced efficiently by EPOC. A novel electrochemically assisted NO_x storage/reduction catalyst was recently reported [58] by de Lucas-Consuegra that can operate over a range of reaction conditions for the effective removal of NO_x. Very interestingly in this system an electro-promotional and a NO_x trapping phenomenon can simultaneously occurred. NO_x is stored on the catalyst surface in form of potassium nitrates under negative polarization while under positive polarization, the catalyst is regenerated, and the stored nitrates are efficiently desorbed and reduced to N_2. The variation of the current under the applied polarizations allowed monitoring the progress of both the storing and the regeneration phases.

It is worth noting that many efforts focus their attention on utilizing new types of solid electrolytes for better performance under EP conditions. Typical examples are the electrolytes studied by the group of Metcalfe exhibiting either H^+ [41] or mixed electronic-ionic [40, 67, 68] conductivity. The variety of H^+ conductors investigated is shown in Table 1, in the studies reported by Thursfield et al. [39], Karagiannakis et al. [65, 69] and Kokkofitis et al. [59, 70, 71].

3 Mechanistic studies and origin of electrochemical promotion of catalysis

The rationalization and the necessity to understand the origin and mechanism of EPOC led during the last 7 years many groups to pay attention in this field too. Besides the results which have been already reported in the literature till 2001 and reviewed by Professor Vayenas et al. in the ''Electrochemical Promotion of Catalysis'' book [28] several new studies have been reported till the end of 2008 using various techniques and methods such as TPD [29, 30, 32, 47, 72], TPR [29], CV [21], FTIR [21], SEM-EDX [21], AC impedance spectroscopy [39], STM [73, 74], work function measurements and theoretical considerations [18, 75, 76], transients experiments and kinetic studies [34, 35], quantum mechanical calculations and Monte Carlo simulations [77] and general thermodynamic considerations [18, 78, 79]. The use of oxygen temperature programmed desorption both under UHV and atmospheric pressure conditions has proven [29, 30] the existence of two different and distinct oxygen adsorption states on the catalyst surface when oxygen ion conductors used like YSZ. As it has been already discussed in Fig. 2, non-stoichiometric oxygen from the solid electrolyte (O^{2-}) adsorbs on the catalyst surface more strongly than oxygen originating from the gas phase. The simultaneous existence of these species ($O^{\delta-}$) on the surface with gas supplied O leads to the sacrificial promoter role for the reaction of electron acceptor adsorbed species (for example O from the gas phase) by forcing them via repulsive lateral interactions to weakly bonded and therefore more reactive sites. The existence of these two well distinguished oxygen states on a electropromoted catalyst surface has been also proven by Li et al. [47] using YSZ as the solid electrolyte and real EPOC atmospheric pressure operation conditions during the TPD study. The observed very strong similarity between O_2 TPD spectra of electrochemically promoted Pt/YSZ films and nanodispersed Pt/YSZ powder catalysts observed in [30] corroborates the mechanistic equivalence of EPOC and metal support interactions (MSI) with O^{2-}-conducting supports something which was an assumption during the first years of EPOC. Recently Vayenas [79] analyzed the EPOC phenomenon from a thermodynamic point of view. He explains how thermodynamics dictates the existence of two oxygen species on the catalyst-electrode surface under

EPOC conditions, one which can, under certain conditions, be equilibrated with the solid electrolyte and controlled by an external applied potential and another having a chemical potential not exceeding that of oxygen in the gas phase (Tables 2, 3, 4).

The in situ change of the work function of a catalyst is the main reason for the modification of catalytic activity and selectivity. Since 1990 it has been proposed [80, 81] that the work function of a gas exposed electrode surface of porous metal films deposited on a solid electrolyte can be varied by at least up to 1 eV by varying the working (W) potential with respect to a reference (R) electrode (U_{WR}) according to equation:

$$\Delta\Phi_W = e\Delta U_{WR} \quad (4)$$

where e is the elementary charge and ΔU_{WR} is the ohmic-drop-free change in the working electrode potential, induced either by changing the gaseous composition or by using a potentiostat or galvanostat in a solid electrolyte cell. Equation 4 has been confirmed in the past by several techniques (PEEM, Kelvin probe technique and UPS) [28]. Despite the fact that the major part of these studies has been already reviewed [28] a noteworthy progress was taken place during the last 7 years. Riess and Vayenas in 2003 [78] discussed the spatial distribution of the electrochemical potential of electrons and of electrostatic potential in solid electrolyte cells without and with ion spillover on the gas-exposed electrode surfaces. In the latter case, where, over a wide temperature range, the spillover ions form an effective double layer at the electrode–gas interface, it was shown both via an electrochemical and a surface science approach, that the solid electrolyte cells are work functions probe and work function controllers for their gas-exposed electrode surfaces, in agreement with experiment. Under these conditions the work function of the working electrode is fixed by the applied potential and not by the gas phase at the working electrode. The above correlation between the work function changes and the catalyst working electrode potential was the subject of two other studies by Leiva et al. [18, 75] published in 2003 and 2007. It has been found that the changes of the work function, $\Delta\Phi$, at the metal/gas interface and the changes of the potential difference, $e\Delta E$, at the metal/solid electrolyte interface are given by the same equation, which contains the changes of the concentrations of ionic species. Furthermore the same group (Leiva et al. [77]) in a very recent study used quantum mechanical calculations and Monte Carlo Grand Canonical simulations in order to simulate the effective double layer occurring on a catalyst surface under EP conditions. Considering solid electrolytes with Na^+ and O^{2-} conductivity and Pt(111) surface they found that Na and O adsorbates show opposite trends concerning the relaxation of the Pt lattice upon adsorption. Na seems to generate an expansion of the Pt lattice caused by the electron transfer to the metal while O induces a compression due to the opposite effect [77].

The origin of EPOC with K^+ conductors was study thoroughly by de Lucas-Consuegra et al. in 2007 [21] studying the mechanism of the low temperature C_3H_6 oxidation over Pt/β''-Al_2O_3 (K^+) via Cyclic Voltammetry, FTIR and SEM-EDX. The presence of more stable and effective promoter phases (potassium oxides and superoxides) was responsible for both permanent NEMCA effect and for the stronger promotional phenomenon in comparison to sodium conductors. The later case of permanent NEMCA where the catalytic rate is not returning to its initial value after current or potential interruption is another interesting feature of NEMCA studied and rationalized firstly by the group of Comninellis in the late 1990s [82]. This group was also the first which introduced the ratio γ, describing the fraction of the permanent modification of catalytic activity, by:

$$\gamma = r'/r_o \quad (5)$$

where r_o is the catalytic rate before the polarization and r' the rate after the polarization interruption at the new steady state conditions. Recently Falgairette et al. [83] studied the phenomenon of permanent electrochemical promotion using Pt/YSZ/Pt electrodes. According to their results the prolonged anodic polarization, in parallel to the reaction of oxygen evolution, causes storage of Pt–O. The majority of these species is released at the tpb, spills over the catalyst/gas interface and promotes the catalytic activity. A part of Pt–O however is stored at two distinct locations, either in situ or in the neighboring Pt phase reached by solid state diffusion, both being hidden from the reactive gas phase. After the interruption of polarization these hidden species reappear at the three phase boundaries (tpb) and spread over the gas-exposed surface thus causing non-Faradaic promotion. The large amount of stored charge and its slow diffusion-controlled emergence causes the rate enhancement to last for several hours.

Another major issue addressed the scientific community of EPOC was the role of the preparation method on the thickness and morphology of the catalyst electrode. For years one of the basic questions was the suitable thickness of the electrode for an optimum behaviour under electropromoting condition. The required low cost of a possible working electrode together with the maximum dispersion could lead to the utilization of thin films but the question was if such films could be promoted under EP conditions. The first theoretical approach was done from Vayenas and Pitselis in 2001 [84] trying to answer the above question. It has been shown theoretically, and a one-dimensional model was developed for this purpose, that the thinner the catalyst-working electrode is the higher enhancement ratio will

Table 2 Studies reported from 2002–2008 on the mechanism and origin of electrochemical promotion of catalysis using several techniques

Mechanistic studies and origin of electrochemical promotion of catalysis				
Study	Technique	Electrocatalyst	General conclusions	References
Oxygen adsorption under Ultra High Vacuum conditions	TPD	Pd/YSZ/Au	Confirmation of two oxygen states on Pd. O^{2-} act as promoters only when applied on a surface with low oxygen coverage	[32]
Fermi level and potential distribution in solid electrolyte cells with and without ion spillover	Thermodynamic considerations	Metal/oxygen ion conductor	The creation of an overall neutral effective electrochemical double layer n the gas exposed electrode surfaces in solid electrochemistry has two consequences: it makes the outer potentials of both electrodes zero and it allow the work functions of the electrodes to vary, due to the varying coverages of the spillover ion. The above lead to the experimental equation, $eU_{WR} = \Phi_W - \Phi_R$	[78]
Corellation between the work function changes and the catalyst working electrode potential	Electrochemical Cell modeling and thermodynamic considerations based on the concept of the absolute electrode potential given by Trasatti [103, 104]	Metal/solid electrolyte	The changes of the work function $\Delta\Phi$ at the metal/gas interface and the changes of the potential difference $e\Delta E$ at the metal/solid electrolyte interface are given by the same equation, which contains the changes of the concentrations of ionic species	[18] [75]
Simulation of the effective double layer under EP conditions	Quantum mechanical calculations and Monte Carlo Grand Canonical simulations	Na/Pt(111) and O/Pt(111)	Na and O adsorbates show opposite trends concerning the relaxation of the Pt lattice upon adsorption. Na seems to generate an expansion of the Pt lattice caused by the electron transfer to the metal while O induces a compression due to the opposite effect	[77]
Low-temperature C_3H_6 combustion	CV, FTIR, SEM-EDX	Pt/β''-Al_2O_3 (K^+)/Au	The present of more stable and effective promoter phases (potassium oxides and superoxides) are responsible for both permanent NEMCA effect and higher promotional phenomenon in comparison to sodium conductors	[21]
Oxygen adsorption under real operating conditions	TPD under UHV	Pt/YSZ/Au	O^{2-} act as effective promoters being on catalyst surface at strongly bonded states in comparison to gas phase oxygen	[47]
The effect of catalyst film thickness on EP. C_2H_4 oxidation	Transients experiments, kinetic studies	Pt/YSZ/Au	A decrease in the rate enhancement ration ρ observed by increasing the thickness of the catalyst film	[34, 35]
Work function changes of polarized electrodes	Work Function measurements	Metal/oxygen conductor	In the case of O^{2-} spillover a moderate equilibrium surface coverage and a reasonable number of surface sites indeed yield the often discussed relationship $\Delta\Phi \approx e\eta$	[76]
Isotope oxygen, $^{18}O_2$, adsorption under Ultra High Vacuum conditions	TPD under UHV	Pt/YSZ/Au	Confirmation of two oxygen states on Pt. O^{2-} adsorb strongly on the surface and force adsorbed oxygen from the gas phase to more weakly (more active) bonded sites	[30]
CO oxidation by isotope oxygen High Vacuum conditions	TPR under HV	Pt/YSZ/Au	Lattice oxygen plays a key role in the oxidation reaction, acting both as a reactant and as a sacrificial promoter. Sacrificial promoter model of electrochemical promotion and metal–support interactions with O^{2-}-conducting supports was confirmed	[29]
Ethylene oxidation using a proton conductor	AC impedance spectroscopy	Pt/BCN/Au	In situ AC impedance spectra reveal a buildup of sacrificial promoter, most likely OH formed by reaction of spillover protons with chemisorbed oxygen	[39]

Table 2 continued

Mechanistic studies and origin of electrochemical promotion of catalysis				
Study	Technique	Electrocatalyst	General conclusions	References
Thermodynamic analysis of EPOC	Thermodynamic considerations	Metal/oxygen conductor	Thermodynamics dictates the existence of two oxygen species on the catalyst electrode surface, one which can be equilibrated with the solid electrolyte, the other having a chemical potential not exceeding that of oxygen in the gas phase. The chemical potential of the former type of oxygen is controlled by the applied potential	[79]
TPD study form the use of fuel cell type reactor	Oxygen TPD using fuel cell type configuration	LSM/YSZ/LaAlO	By applying external potential the amount of adsorbed oxygen on the anode catalyst is altered and the activation energy of desorption is decreased. A correlation between the behaviour of adsorbed oxygen species and the change in the selectivity of oxidative coupling of methane in SOFC reactor is also observed	[72]
STM observation of the origin of electrochemical promotion and metal-support interactions	STM under atmospheric pressure	Pt(111)/YSZ/Au and Pt(111)/β''-Al_2O_3(Na^+)/Au	STM images have positively confirmed the electrochemically assisted O^{2-} and Na^+ migration (backspillover) on the Pt(111) surfaces interfaced with YSZ and β''-Al_2O_3. Mechanistic similarity of EP and MSI was also confirmed	[73, 74]
Study of permanent EPOC	CV, LSV, transient experiments	Pt/YSZ/Pt	The prolonged anodic polarization causes storage of Pt–O. The majority of these species is released at the tpb, spills over the catalyst/gas interface and promotes the catalytic activity. A part of Pt–O however stored is hidden from the reactive gas phase regions, reappears at tpb after the interruption of polarization, this causing the P-EPOC	[83]

Table 3 Studies reported from 2002–2008 on the commercialization of electrochemical promotion of catalysis

Studies on the commercialization of electrochemical promotion of catalysis					
Reactants	Reaction type	Reactor type	Electrocatalyst	General behaviour under EP conditions	References
NO, C_2H_4, O_2	Reduction	MEPR (22 plates)	Rh/YSZ/Pt	NO reduction enhancement by 450% with almost 100% selectivity to N_2 and Λ values up to 2.4	[86, 87, 89]
NO, C_2H_4, O_2	Reduction	MEPR (8 plates)	Pt–Rh/YSZ/Au	Inverted volcano behaviour. 50% fuel and 44% NO rate enhancements at 335 °C in presence of up to 10% O_2 and high flowrates	[88]
C_2H_4, O_2	Oxidation	Wireless Reactor	Pt/LSC/Pt	One order of magnitude promotion of the reaction by inducing an oxygen chemical potential difference across the membrane	[67, 68]
C_2H_4, O_2	Oxidation	MEPR (2 or 10 plates)	Rh/YSZ/Pt	Ethylene conversion increase from 19% to 43.5% while NO conversion increases from 30.5% to 56% under positive polarization at 300 °C	[86, 87]
Real car exhausts	Oxidations reductions	MEPR (21 plates)	Rh/YSZ/Pt	Apply of negative potential causes an increase both in NO and NO_x conversion. Electro- promotion has about the one forth of the impact of fuel injection	[91]

Table 4 Studies reported from 2002–2008 on the application of electrochemical promotion of catalysis to low and high temperature fuel cell devices

Application of EPOC in high or low temperature fuel cell devices				
Reactants	Reaction type	Electrocatalyst	General behaviour under EP conditions	References
PEMFC Anode: CO_2, H_2, CO, N_2,O_2 Cathode: Air or H_2	WGS reaction, CO oxidation	Pt/Nafion 117/Pt, Pt/Nafion 1135/Pt and Pt–Cu/Nafion 117/Pt	Electrochemical Promotion observed under normal fuel cell and O_2 bleeding operation while sub-Faradaic behaviour was observed in absence of oxygen (hydrogen pumping operation)	[95, 96]
SOFC Anode: H_2, C_2H_6, CH_4 Cathode: Air	H_2 C_2H_6 or CH_4 oxidation (triode operation)	SOFC Pt/YSZ/Pt	Application of the triode operating mode to SOFC and CO-poisoned PEMFC can decrease electrode polarization losses and permit the use of alternative less costly electrode materials	[97, 98]
PEMFC Anode: H_2, CO Cathode: Air		PEMFC Pt–Ru/Nafion 117/Pt		
PEMFC Anode: H_2 Cathode: olefins	Isomerization of 2-3-dimethyl-1-butene and 3-3-dimethyl-1-butene	Pd/C/Nafion 117/Pt	The isomerization of 2-3-dimethyl-1-butene was enhanced over a thousand fold ($\rho = 1230$) by proton spillover on the carbon supported Pd catalyst	[94]

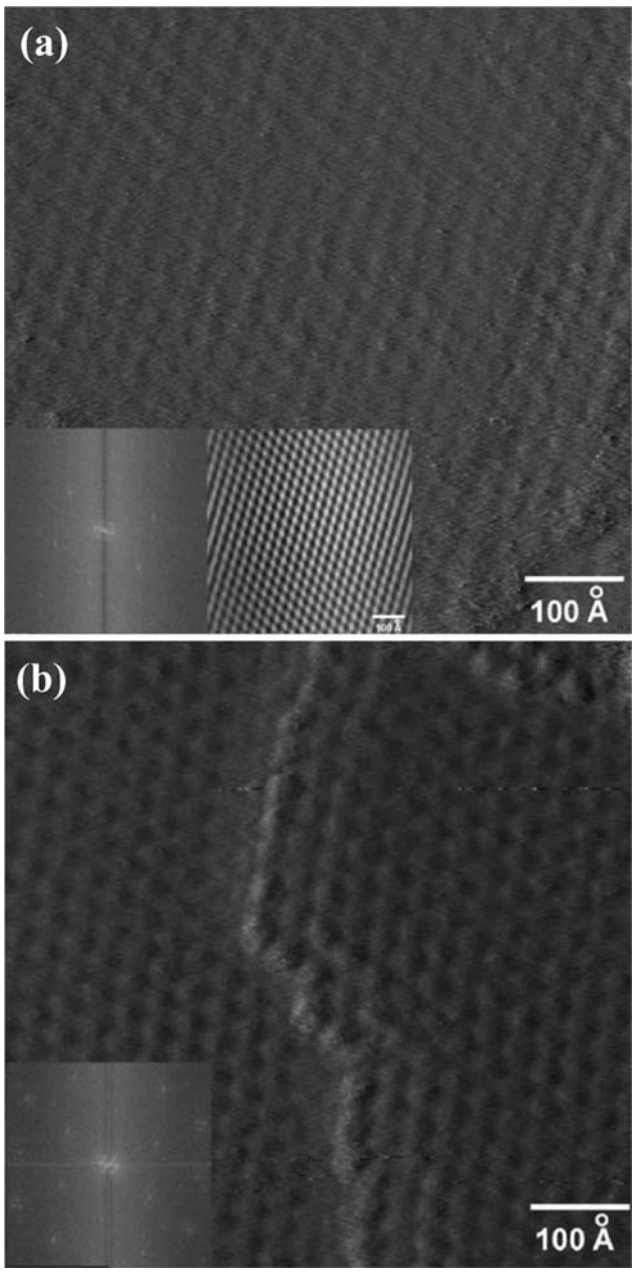

Fig. 6 Electrochemically promoted single crystals. **a** Unfiltered STM image of the Pt (111) surface of the Pt(111)/YSZ system following positive potential application ($U_{WR} = 1$ V) showing the backspillover O^{2-} formed Pt(111)-(12 × 12)-O adlattice overlapping with the underlying Pt(111)-(2 × 2)-O adlattice. Inset shows the Fourier transform spectrum and the corresponding filtered image ($U_t = 0.4$ V, $I_t = 8$ nA) [74] and **b** Unfiltered STM image of the Pt(111) surface of the Pt(111)/β''-Al_2O_3 system following a negative current application ($I = -5$ μA) showing the backspillover Na^+ formed Pt(111)-(12 × 12)-Na adlattice overlapping with the underlying Pt(111)-(2 × 2)-O adlattice. Inset shows the Fourier transform spectrum ($U_t = -0.16$ V, $I_t = 10$ nA) [74]. Reprinted with permission from Elsevier

be observed. Experimental validation for the above model came 5 years later by Koutsodontis et al. [34, 35] using several Pt/YSZ electrocatalysts with various Pt loadings, catalyst thickness and different methods of preparation. In these two studies the effect of catalyst film thickness on the magnitude of the effect of electrochemical promotion was investigated for the model catalytic reaction of C_2H_4 oxidation. It was found that the catalytic rate enhancement ρ is up to 400 for thinner (0.2 μm) Pt films (40,000% rate enhancement) and gradually decreases to 50 for thicker films (1 μm). The Faradaic efficiency Λ was found to increase moderately with increasing film thickness and to be described semiquantitatively by the ratio $2Fr_o/I_o$, where r_o is the unpromoted rate and I_o is the exchange current of the catalyst–electrolyte interface. The results were in good qualitative agreement with the model predictions [84] describing the diffusion and reaction of the backspillover O^{2-} species, which causes the EP. In previous study [85] the influence of the thickness of sputter-deposited Platinum films on the Electrochemical Promotion of propane combustion was studied by Billard and Vernoux. They found that the catalytic activity does not follow a linear evolution with the film thickness while NEMCA measurements performed at 337 °C and 400 °C indicate that a minimal thickness of about 15 nm is required in order to allow the bias of the whole Pt surface.

Very interesting results on the origin of EPOC were reported also using the technique of STM under atmospheric pressure and ambient conditions [73, 74]. The surface of a Pt(111) single crystal well attached with YSZ (O^{2-} conductor) [73, 74] and β''-Al_2O_3 (Na^+ conductor) [74] was investigated both under open circuit, cathodic and anodic polarization. The results confirm the reversible electrochemically controlled backspillover of sodium and of O^{2-} between the solid electrolyte and the Pt(111) surface but also the mechanism of EP and MSI. Anodic polarization causes the decoration of the Pt single crystal surface interfaced with the YSZ support with O^{2-} species (Fig. 6a). These species form a Pt(111)-(12 × 12)-O adlatttice which coexists with the familiar Pt(111)-(2 × 2)-O adlattice formed by gaseous oxygen (Fig. 6a). Equivalently, cathodic polarization covers the Pt(111) surface with Na^+ in the case of β''-Al_2O_3 support (Fig. 6b). According to Archonta et al. [74] and their results the above backspillover phenomenon can also take place due to thermal diffusion of O^{2-} or Na^+ under open circuit conditions, something which is happening in commercial dispersed catalysts too, since in such catalysts the metal crystallites are much smaller and thus the diffusion length much shorter.

4 Practical application of EPOC

Although EPOC has been studied using over eighty different catalytic systems, until recently there has been no large-scale commercial utilization mainly for two reasons:

(a) Expensive thick catalyst films (typically 0.1–5 μm thick) with metal dispersion below 0.01%.
(b) Lack of efficient and compact reactor designs allowing for the utilization of EP with a minimum of electrical connections to the external power supply.

In 2004 [86] the group of Vayenas reported the first large-scale application of EPOC as a result of their efforts to overcome the above limitations. A novel monolithic reactor was developed capable to carry many electrochemical cells and handle high flowrates of reactants (Fig. 7). The reactor which can be considered as a hybrid between a classical monolithic honeycomb reactor (of which it has all the geometric dimensions) and of a flat- or ribbed-plate solid oxide fuel cell, consists of flat or ribbed solid electrolyte plates (Fig. 7), covered on both sides by appropriate thin porous conductive catalyst layers (prepared via sputtering). The plates are inserted in appropriately carved grooves on the inside surfaces of the walls of the ceramic reactor casing. These surfaces are also used to create two current collectors, one establishing electrical contact among all catalyst films deposited on the top side of the plates, the other current collector establishing electrical contact with all catalyst films deposited on the bottom side of the plates (Fig. 7). In this way, all catalyst films could be electrochemically promoted via only two external connecting wires (Fig. 8). This was a significant practical simplification for the commercialization of EPOC. Besides, the metal dispersion of the prepared thin sputtered noble metal electrodes was higher than 15% [86]. Contrary to the case of fuel cells, where the fuel and air gas streams are kept separated, in the case of the MEP reactor, similar to the case of single chamber fuel cells, conceptually there is only one gas stream containing all reactants and products, as in every classical catalytic reactor. An additional advantage of the MEP reactor is that it can be assembled and dismantled at will and its flat or ribbed plates can be replaced whenever necessary. Also it is possible to use one of the plates as a gas-sensor element and utilize the potential signal generated by this element, under open-circuit or at a fixed applied current, to control the current or potential applied to the electropromoted catalytic plates.

Many studies have already been published [86–90] after the first report of MEPR [86] showing its advantages for several reaction (oxidations, reductions, hydrogenations etc.). In a very recent report [89] the reaction of NO by

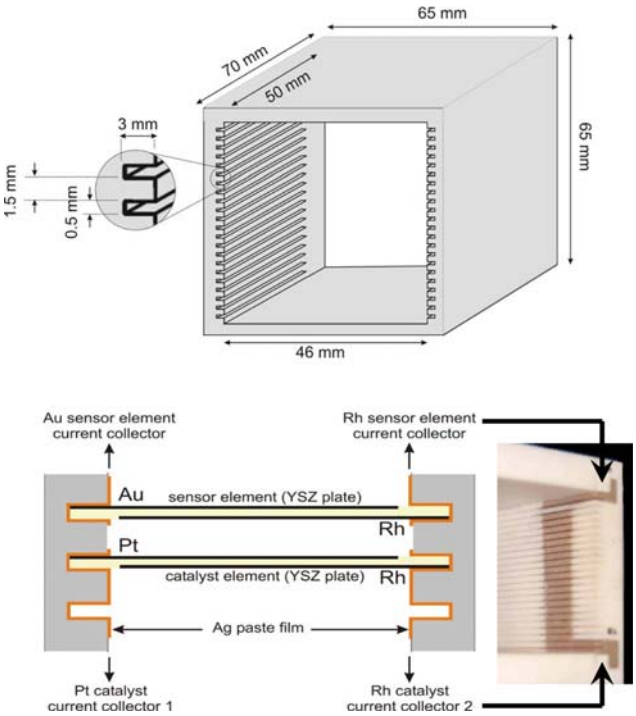

Fig. 7 Schematic and dimensions of the monolithic electropromoted reactor (MEPR) capable to carry up to 22 flat or ribbed electrochemical plates (*up*). The geometry of the electrical connections on the MEP reactor ceramic walls (*down*) [86]. Reprinted with permission from Elsevier

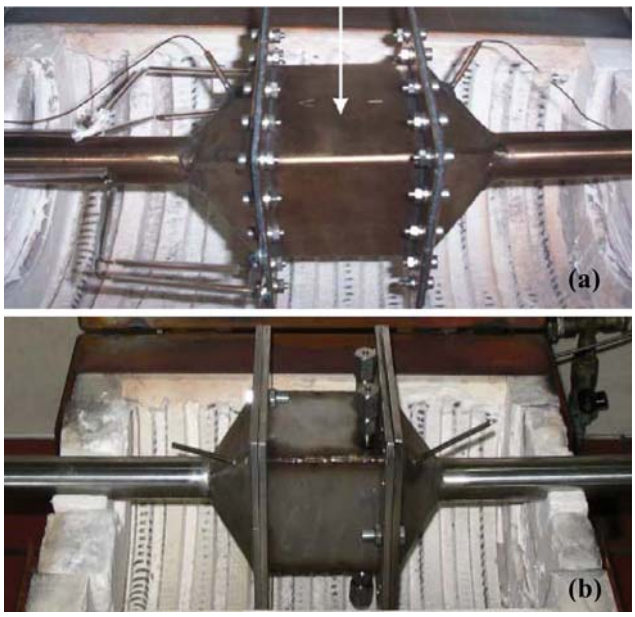

Fig. 8 Photographs of the MEPR showing **a** the first generation reactor developed in 2004 [86] and **b** the latest version of the reactor with better sealed components and minimum number of electrical connections. Reprinted with permission from Elsevier

C_2H_4 in high excess of O_2 and low temperatures (200–300 °C) was investigated using a new improved version of MEPR (with better sealing, Fig. 8b) by Souentie et al. Twenty two Rh/YSZ/Pt parallel plate elements were used in the reactor under flowrate up to 1lt/min and various gaseous feed compositions (near stoichiometric oxygen, medium oxidizing and highly oxidizing conditions). Figure 9 shows anodic galvanostatic transient obtained in a slightly oxidizing C_2H_4–NO–O_2 mixture, where the O_2 excess (defined as $y_{O_2} + 1/2y_{NO} - 3y_{C_2H_4}$) [89] is 0.08% and lamda value λ (expresses the O_2/fuel ratio present in automotive exhaust) is 1.12. Upon positive current imposition (+30 mA, e.g. O^{2-} supply to Rh) surface the ethylene conversion increases from 26% to 78% ($\rho_{CO_2} = 2.8$), the O_2 conversion increases from 29% to 83%, while the NO conversion increases from 28% to 94% ($\rho = 3.37$). Furthermore, the effective enhancement ratio, ρc (defined as ρ/ρ_{max}) for the CO_2 production rate is 0.78, while for the NO reduction rate it reaches 0.94, which means that the achieved NO conversion via the NEMCA effect is 94% of the maximum possible conversion (100%). No measurable concentration of N_2O was found in the products and thus N_2 was the only measurable product of the reduction of NO. Also no measurable concentration of NO_2 was detected. The observed high selectivity to N_2 implies that all N_2O possibly produced by NO reduction on the Pt catalyst-electrodes is further reduced to N_2 on the Rh catalyst-electrodes. The phenomenon is reversible, since current interruption causes both rates to return to their initial values after approximately 70 min (Fig. 9). Until today the MEPR reactor was used mainly for NO reduction by C_2H_4 and C_2H_4 oxidation while studies on SO_2 oxidation and CO_2 hydrogenation using Rh/YSZ/Pt and Cu/TiO_2/YSZ/Au electrochemical plates are currently under way. It is worth noting that the operation of the above reactor with 21 Rh/YSZ/Pt electrochemical plates has also studied once under real car exhaust conditions [91]. These preliminary results show that application of negative potential (e.g. O^{2-} supply to Pt) causes an increase both in NO and NO_x conversion. Electropromotion under the above conditions had about the one fourth of the effect of fuel injection [91]. This is quite encouraging for further future applications.

Another approach for scaling up EPOC and overcoming problems regarding electrical connections was proposed by the group of Metcalfe. Poulidi et al. in recent studies [67, 68, 92] introduce the term of wireless EPOC. The concept is based on the utilization of fuel cell type configurations and the control of oxygen chemical potential difference across the solid electrolyte. In a recent study [68] a LSCF mixed ionic electronic conductor membrane was used for the promotion of the catalytic activity of a Pt catalyst during ethylene oxidation. By controlling the oxygen chemical potential difference, a driving force for oxygen

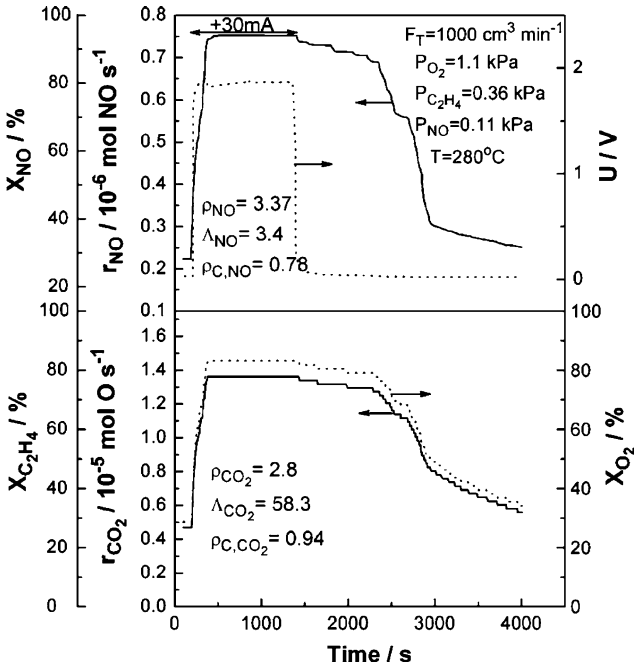

Fig. 9 Transient effect of a constant applied current (+30 mA) on the catalytic rate of NO reduction (r_{NO}) and CO_2 formation (r_{CO_2}), on the NO, C_2H_4 and O_2 conversion (X_{NO}, $X_{C_2H_4}$, X_{O_2}) and on the Rh-Pt potential difference (U). $T = 280$ °C [89]. Reprinted with permission from Springer

ions to migrate across the membrane and backspillover onto the catalyst surface is established. In this way the reaction is promoted according to EPOC rules by the formation of a double layer of oxide ions on the catalyst surface. The electronic conductivity of the membrane material eliminates the need for an external circuit to pump the promoting oxide ion species making the concept simpler and more amenable for large scale practical application. The results [68] show that the reaction rate of ethylene oxidation can indeed be promoted significantly upon exposure to an oxygen atmosphere on the sweep side of the membrane reactor, and thus inducing an oxygen chemical potential difference across the membrane, as compared to the rate under an inert sweep gas.

5 Application of EPOC on high or low temperature fuel cell devices

Both low (PEMFC) and high (SOFC) temperature fuel cells have been used during the last 7 years as reactors (co-generators) for specific reactions under electropromoted conditions. The first paper reported in literature exploiting the application of EPOC on the performance of a normal PEMFC under electropromoted conditions (proton spillover) was in 1997 dealing with the isomerization of

n-butylenes [9]. Another example reported from the same group of Smotkin was already analyzed in the introduction (Fig. 4) regarding the isomerization of 1-butene to cis-2-butene and trans-2-butene on nanodispersed Pd/C catalyst deposited on porous conductive graphitic C supported on Nafion [93]. Recently Salazar and Smotkin [94] reported electrochemically promoted olefin isomerization reactions using similar electrocatalysts (Pd as cathode and Pt as anode) in a polymer electrolyte fuel cell. The isomerization of 2-3-dimethyl-1-butene to 2-3-dimethyl-2-butene was enhanced over a thousand fold ($\rho = 1230$) by spillover of protons generated by low currents on carbon supported Pd catalyst [94]. The same type of low temperature fuel cell has been also used by Sapountzi et al. in 2007 [95, 96] in order to examine the possibility of electrochemically promoting the CO oxidation and water gas shift (WGS) reaction and therefore making a gas mixture produced from a methanol reformate unit (containing CO, CO_2, N_2 and H_2) suitable for anodic oxidation. Using several type of MEAs (Pt/Nafion 117/Pt, Pt/Nafion 1135/Pt and Pt–Cu/Nafion 117/Pt) it was found that the electrochemical promotion effect plays a significant role in a normal fuel cell operation (air at the cathode) but not in the hydrogen pumping operation (H_2 at the cathode). This observation can imply the importance of oxygen crossover in the electropromotion of the WGS reaction and of the CO oxidation.

A novel idea in the field of fuel cell electropromotion was introduced in 2004 by the group of Vayenas [97] by proposing the triode fuel cell operation. In addition to the anode and cathode the new device introduces a third electrode together with an auxiliary circuit which is running in the electrolytic mode and permits fuel cell operation under previously inaccessible anode–cathode potential differences (Fig. 10). Studies using either low (PEMFC) or high (SOFC) temperature fuel cells have been curried out [97, 98] showing that both the power output can be enhanced (by up to a factor of 8) and the overall efficiency can also be improved via application of electrolytic currents between the anode or cathode and the third auxiliary electrode.

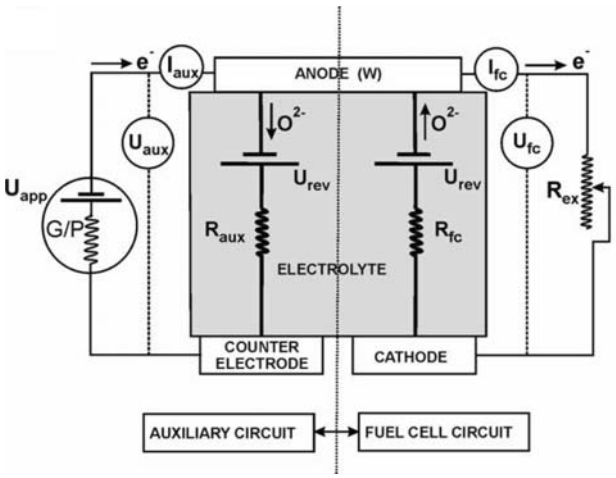

Fig. 10 Schematic of triode fuel cell concept. Fuel cell anode acts simultaneously as the working electrode of the auxiliary circuit. G/P: galvanostat–potentiostat [97]. Reprinted with permission from The Electrochemical Society

6 Conclusions

Many studies have been published during the last 7 years regarding the effect of the Electrochemical Promotion of Catalysis, its origin and application to several types of reactions with environmental and industrial interest. The effectiveness of EPOC for catalytic oxidations, reductions, hydrogenerations, decompositions, and isomerizations using numerous types of solid electrolytes and catalysts underlines the importance of this phenomenon both in catalysis and electrochemistry. The utilization of EPOC in fuel cells also appears quite promising and worth further investigation. The development of new monolithic reactors with compact design and minimization of the electrical connections and the use of wireless configurations may contribute to practical applications of EPOC.

References

1. Stoukides M, Vayenas CG (1981) J Catal 70:137
2. Politova TI, Sobyanin VA, Belyaev VD (1990) React Kinet Catal Lett 41:321
3. Foti G, Wodiunig S, Comninellis C (2000) Curr Top Electrochem 7:1
4. Harkness I, Lambert RM (1995) J Catal 152:211
5. Cavalca CA, Haller GL (1998) J Catal 177:389
6. Anastasijevic NA, Hillrichs E, Lohrberg K, Ungar G (1997) US Patent
7. Stoukides M (1988) Ind Eng Chem Res 27:1745
8. Yentekakis IV, Lambert RM, Tikhov MS, Konsolakis M, Kiousis V (1998) J Catal 176:82
9. Ploense L, Salazar M, Gurau B, Smotkin ES (1997) J Am Chem Soc 119:11550
10. Douvartzides SL, Tsiakaras PE (2002) J Catal 211:521
11. Poppe J, Voelkening S, Schaak A, Schuetz E, Janek J, Imbihl R (1999) Phys Chem Chem Phys 1:5241
12. Pacchioni G, Lomas JR, Illas F (1997) Mol Catal A Chem 119:263
13. Petrushina IM, Bandur VA, Cappeln F, Bjerrum NJ (2000) J Electrochem Soc 147:3010
14. Hong JK, Oh I-H, Hong S-A, Lee WY (1996) J Catal 163:95
15. Emery DA, Middleton PH, Metcalfe IS (1998) Surf Sci 405:308
16. Janek J, Rohnke M, Luerssen B, Imbihl R (2000) Phys Chem Chem Phys 2:1935
17. Lamy-Pitara E, Mouahid SE, Barbier J (2000) Electrochim Acta 45:4299
18. Leiva EPM, Sanchez CG (2003) J Solid State Electrochem 7:588

19. Vernoux P, Gaillard F, Bultel L, Siebert E, Primet M (2002) J Catal 208:412
20. de Lucas-Consuegra A, Dorado F, Jimenez-Borja C, Valverde JL (2008) Appl Catal B Environ 78:222
21. de Lucas-Consuegra A, Dorado F, Valverde JL, Karoum R, Vernoux P (2007) J Catal 251:474
22. Bockris JOM, Minevski ZS (1994) Electrochim Acta 39:1471
23. Lu G-Q, Wieckowski A (2000) Curr Opin Colloid Interface Sci 5:95
24. Pritchard J (1990) Nature 343:592
25. Grzybowska-Swierkosz B, Haber J (1994) In: Annual reports on the progress of chemistry, The Royal Society of Chemistry, Cambridge
26. Riess I (2006) Solid State Ionics 177:1591
27. Riess I (2005) Solid State Ionics 176:1667
28. Vayenas CG, Bebelis S, Pliangos C, Brosda S, Tsiplakides D (2001) In: Electrochemical activation of catalysis: promotion, electrochemical promotion and metal-support interactions, Kluwer Academic/Plenum Publishers, New York
29. Katsaounis A, Nikopoulou Z, Verykios XE, Vayenas CG (2004) J Catal 226:197
30. Katsaounis A, Nikopoulou Z, Verykios XE, Vayenas CG (2004) J Catal 222:192
31. Neophytides S, Tsiplakides D, Vayenas CG (1998) J Catal 178:414
32. Katsaounis A (2008) J Appl Electrochem 38:1097
33. Bebelis S, Vayenas CG (1989) J Catal 118:125
34. Koutsodontis C, Katsaounis A, Figueroa JC, Cavalca C, Pereira C, Vayenas CG (2006) Top Catal 39:97
35. Koutsodontis C, Katsaounis A, Figueroa JC, Cavalca C, Pereira CJ, Vayenas CG (2006) Top Catal 38:157
36. Bebelis S, Kotsionopoulos N (2006) Solid State Ionics 177:2205
37. Kokkofitis C, Karagiannakis G, Zisekas S, Stoukides M (2005) J Catal 234:476
38. Roche V, Karoum R, Billard A, Revel R, Vernoux P (2008) J Appl Electrochem 38:1111
39. Thursfield A, Brosda S, Pliangos C, Schober T, Vayenas CG (2003) Electrochim Acta 48:3779
40. Poulidi D, Metcalfe IS (2006) Solid State Ionics 177:2211
41. Poulidi D, Castillo-del-Rio MA, Salar R, Thursfield A, Metcalfe IS (2003) Solid State Ionics 162–163:305
42. Karoum R, de Lucas-Consuegra A, Dorado F, Valverde JL, Billard A, Vernoux P (2008) J Appl Electrochem 38:1083
43. Gaillard F, Li XG, Uray M, Vernoux P (2004) Catal Lett 96:177
44. Vernoux P, Gaillard F, Lopez C, Siebert E (2004) Solid State Ionics 175:609
45. Billard A, Vernoux P (2007) Top Catal 44:369
46. Roche V, Siebert E, Steil MC, Deloume JP, Roux C, Pagnier T, Revel R, Vernoux P (2008) Ionics 14:235
47. Li X, Gaillard F, Vernoux P (2007) Top Catal 44:391
48. Kotsionopoulos N, Bebelis S (2007) Top Catal 44:379
49. Kotsionopoulos N, Bebelis S (2005) J Appl Electrochem 35:1253
50. Kokkofitis C, Karagiannakis G, Stoukides M (2007) Top Catal 44:361
51. Tsiakaras PE, Douvartzides SL, Demin AK, Sobyanin VA (2002) Solid State Ionics 152:721
52. de Lucas-Consuegra A, Dorado F, Valverde JL, Karoum R, Vernoux P (2008) Catal Commun 9:17
53. Lintanf A, Djurado E, Vernoux P (2008) Solid State Ionics 178:1998
54. Vernoux P, Gaillard F, Karoum R, Billard A (2007) Appl Catal B Environ 73:73
55. Dorado F, de Lucas-Consuegra A, Vernoux P, Valverde JL (2007) Appl Catal B Environ 73:42
56. Dorado F, de Lucas-Consuegra A, Jimenez C, Valverde JL (2007) Appl Catal A Gen 321:86
57. Vernoux P, Gaillard F, Lopez C, Siebert E (2003) J Catal 217:203
58. de Lucas-Consuegra A, Caravaca A, Sanchez P, Dorado F, Valverde JL (2008) J Catal 259:54
59. Kokkofitis C, Ouzounidou M, Skodra A, Stoukides M (2007) Solid State Ionics 178:475
60. Karagiannakis G, Zisekas S, Stoukides M (2003) Solid State Ionics 162–163:313
61. Skodra A, Ouzounidou M, Stoukides M (2006) Solid State Ionics 177:2217
62. Vayenas CG, Brosda S, Pliangos C (2001) J Catal 203:329
63. Brosda S, Vayenas CG (2002) J Catal 208:38
64. Brosda S, Vayenas CG, Wei J (2006) Appl Catal B Environ 68:109
65. Karagiannakis G, Kokkofitis C, Zisekas S, Stoukides M (2005) Catal Today 104:219
66. Constantinou I, Archonta D, Brosda S, Lepage M, Sakamoto Y, Vayenas CG (2006) J Catal 251:400
67. Poulidi D, Thursfield A, Metcalfe IS (2007) Top Catal 44:435
68. Poulidi D, Mather GC, Metcalfe IS (2007) Solid State Ionics 178:675
69. Karagiannakis G, Zisekas S, Kokkofitis C, Stoukides M (2006) Appl Catal A Gen 301:265
70. Kokkofitis C, Ouzounidou M, Skodra A, Stoukides M (2007) Solid State Ionics 178:507
71. Kokkofitis C, Karagiannakis G, Stoukides M (2007) Catal Today 127:330
72. Kiatkittipong W, Tagawa T, Goto S, Assabumrungrat S, Praserthdam P (2004) Solid State Ionics 166:127
73. Vayenas C, Archonta D, Tsiplakides D (2003) J Electroanal Chem 554–555:301
74. Archonta D, Frantzis A, Tsiplakides D, Vayenas CG (2006) Solid State Ionics 177:2221
75. Leiva EPM (2007) Top Catal 44:347
76. Fleig J, Jamnik J (2005) J Electrochem Soc 152:E138
77. Leiva EPM, Vazquez C, Rojas MI, Mariscal MM (2008) J Appl Electrochem 38:1065
78. Riess I, Vayenas CG (2003) Solid State Ionics 159:313
79. Vayenas CG (2004) Solid State Ionics 168:321
80. Vayenas CG, Bebelis S, Ladas S (1990) Nature 343:625
81. Ladas S, Bebelis S, Vayenas CG (1991) Surf Sci 251/252:1062
82. Nicole J, Tsiplakides D, Wodiunig S, Comninellis C (1997) J Electrochem Soc 144:L312
83. Falgairette C, Jaccoud A, Foti G, Ch C (2008) J Appl Electrochem 38:1075
84. Vayenas CG, Pitselis GE (2001) Ind Eng Chem Res 40:4209
85. Billard A, Vernoux P (2005) Ionics 11:126
86. Balomenou S, Tsiplakides D, Katsaounis A, Thiemann-Handler S, Cramer B, Foti G, Comninellis C, Vayenas CG (2004) Appl Catal B Environ 52:181
87. Balomenou SP, Tsiplakides D, Katsaounis A, Brosda S, Hammad A, Foti G, Comninellis C, Thiemann-Handler S, Cramer B, Vayenas CG (2006) Solid State Ionics 177:2201
88. Koutsodontis C, Hammad A, Lepage M, Sakamoto Y, Foti G, Vayenas CG (2008) Top Catal 50:192
89. Souentie S, Hammad A, Brosda S, Foti G, Vayenas CG (2008) J Appl Electrochem 38:1159
90. Tsiplakides D, Balomenou S, Katsaounis A, Archonta D, Koutsodontis C, Vayenas CG (2005) Catal Today 100:133
91. Balomenou S, Tsiplakides D, Vayenas CG, Poulston S, Houel V, Collier A, Konstandopoulos A, Agrafiotis C (2007) Top Catal 44:481
92. Poulidi D, Metcalfe IS (2008) J Appl Electrochem 38:1121
93. Ploense L, Salazar M, Gurau B, Smotkin ES (2000) Solid State Ionics 136:713
94. Salazar M, Smotkin ES (2006) J Appl Electrochem 36:1237

95. Sapountzi F, Tsampas MN, Vayenas CG (2007) Top Catal 44:461
96. Sapountzi FM, Tsampas MN, Vayenas CG (2007) Catal Today 127:295
97. Balomenou SP, Vayenas CG (2004) J Electrochem Soc 151:A1874
98. Balomenou SP, Sapountzi F, Presvytes D, Tsampas M, Vayenas CG (2006) Solid State Ionics 177:2023
99. Bebelis S, Karasali H, Vayenas CG (2008) Solid State Ionics 179:1391
100. Bebelis S, Karasali H, Vayenas CG (2008) J Appl Electrochem 38:1127
101. de Lucas-Consuegra A, Dorado F, Jimenez-Borja C, Valverde JL (2008) J Appl Electrochem 38:1151
102. Labou D, Neophytides SG (2007) Top Catal 44:451
103. Trasatti S (1990) Electrochim Acta 35:269
104. Trasatti S (1982) J Electroanal Chem 139:1